

Drug Repurposing for Vancomycin-Resistant *Enterococcus faecalis* (V583): A Structure-Based Virtual Screening Approach

Sanjivani Panditkar¹, Machchhindra Holam², Satish Dhonde³, Tushar Fegade^{4*}

¹Department of Applied Chemistry, Yashwantrao Chavan College of Engineering, Affiliated to Rashtrasant Tukadoji Maharaj Nagpur University, Nagpur, Maharashtra, India

²Department of Pharmaceutical Chemistry, Sant Gajanan Maharaj College of Pharmacy, Mahagaon, Affiliated to Shivaji University, Kolhapur, Maharashtra, India

³Department of Pharmacology, SVNH College of B.Pharmacy, Rahuri, Ahilyanagar, Affiliated to Savitribai Phule Pune University, Pune, Maharashtra, India

⁴Department of Pharmaceutics, Shellino Education Society's Arunamai College of Pharmacy, Mamurabad, Affiliated to Kavayitri Bahinabai Chaudhari North Maharashtra University, Jalgaon, Maharashtra, India

Received: 29th Dec, 2024; Revised: 19th Mar, 2025; Accepted: 21st Apr, 2025; Available Online: 25th Jun, 2025

ABSTRACT

Bacterium *Enterococcus faecalis* that has shown resistance against Vancomycin (V583) happens to pose serious threats on the clinical front as it is resistive to the last line of antibiotics drugs. This study looks like a structure-based virtual screening of the predicted inhibitors for AhpF C503A mutant form of the bacteria *E. faecalis*. Such refinement would improve a model that uses the PDB-REDO server which brings down R-free from 22.1% to 19.6% while improving stereochemical accuracy. The refined structure was validated for computational screening by using ProSA, Ramachandran plot analysis, and Verify3D. The receptor-based virtual screening from DrugRep FDA approved drug identified the following compounds with high binding affinity as top-three candidates: Venetoclax (-10.2 kcal/mol), Rimegepant (-9.7 kcal/mol) and Lumacaftor (-9.5 kcal/mol). Key interactions consist of hydrogen bond formations and hydrophobic contacts, as evidenced by the molecular docking analysis within these active sites. Such findings provide potential drug repurposing candidates for *E. faecalis* infections and part of the foundation for further molecular dynamics simulations and experimental validation.

Keywords: Vancomycin-resistant *Enterococcus faecalis*, drug repurposing, structure-based virtual screening, AhpF C503A, molecular docking, PDB-REDO, antimicrobial resistance, FDA-approved drugs

How to cite this article: Sanjivani Panditkar, Machchhindra Holam, Satish Dhonde, Tushar Fegade. Drug Repurposing for Vancomycin-Resistant *Enterococcus Faecalis* (V583): A Structure-Based Virtual Screening Approach. International Journal of Drug Delivery Technology. 2025;15(2):510-18. doi: 10.25258/ijddt.15.2.19

Source of support: Nil

Conflict of interest: None

INTRODUCTION

AMR is an important emerging public health crisis with increased morbidity, mortality, and health care costs associated with infections caused by multidrug-resistant bacteria.¹ One of the more prominent opportunistic pathogens today is *Enterococcus faecalis*, responsible mainly for infections within hospitals.² This Gram-positive bacterium is responsible for a very broad spectrum of clinical conditions, from UTIs to endocarditis, to wound infections, to blood infections, but concerning all of these is the increasing incidence of strains of *Enterococcus faecalis* that exhibit resistance to vancomycin (VRE), such as *E. faecalis* V583, that critically limit therapeutic options in clinical treatment; such rising resistance reveals an urgent need for novel intervention strategies to effectively combat these unyielding infections.³

The first fully sequenced genome of a vancomycin-resistant *Enterococcus*, *E. faecalis* V583, opened the door to the understanding of its resistance mechanisms.⁴ The genomic analysis uncovered many mobile genetic elements like plasmids and transposons that add to its

extensive antibiotic resistance spectrum.⁵ Unlike the other vancomycin-resistant *Enterococcus* strains, the specific strain of *E. faecalis* V583 shows resistance to not only vancomycin but also aminoglycosides, beta-lactams, and tetracyclines and is very difficult to eliminate by conventional antibiotics.⁶ In this regard, multidrug-resistant strains of such persisting and adaptable nature warrant investigations into alternative drug into-the-practice strategies such as drug repurposing.⁷

Drug repositioning or drug repurposing comprises finding an existing FDA-approved drug with another therapeutic use.⁸ This has recently gained traction in antimicrobials as it serves as a cheaper and faster alternative to traditional drug discovery.⁹ Since repurposed drugs have gone through wide-ranging safety and pharmacokinetics measures, they can avoid the entry-stage trials and quickly pivot to a new utility. In an antimicrobial resistance context, drug repurposing affords a quick way of looking for compounds that either foster or hinder bacterial growth by building synergy with the classical antibiotic.¹⁰

*Author for Correspondence: tusharfegade@gmail.com

From this forefront, drug repurposing could be aimed at targeting *E. faecalis* V583¹¹ such molecules that target potent resistance mechanisms, inhibit biofilm formation, or restore susceptibility to antibiotics. Biofilm infections caused by *E. faecalis* V583 are known to be remarkably difficult to treat due to the additional resistance posed by biofilms against antimicrobial agents.¹² Thus, it is also extremely important to screen for repurposed drugs that directly disrupt biofilm formation. Furthermore, the screening and identification of repurposed drugs with the ability to block the major bacterial efflux pumps and any key resistance proteins could reinstate the potency of traditional antibiotics, brightly shining the path to overcome drug resistance in *E. faecalis*.¹³

The Structure-Based Virtual Screening (SBVS), a very much evolved computational tool for drug discovery, targets drug design through study of drug/protein interactions at the molecular level in bacteria.¹⁴ This in silico screening technique enables quick evaluation of thousands of FDA-approved drugs against well-characterized structures of bacterial proteins, maximizing the chances of clicking a therapeutic compound of interest.¹⁵ SBVS is beneficial for antimicrobial discoveries since it precisely maps onto resistance-associated proteins, maximizing opportunities for successful drugs to be repurposed.¹⁶

Table 1: Receptor-based Screen Summary

ID	Name	Score	MW	HBD	HBA	RB	NOA	Rings	LogP
DB11581	Venetoclax	-9.4	868.45	2	6	13	14	8	8.1
DB12457	Rimegepant	-8.9	534.568	1	4	5	9	6	3.5
DB09280	Lumacaftor	-8.5	452.414	2	4	7	7	5	4.4
DB08827	Lomitapide	-8.5	693.7204	2	2	12	5	6	8.6
DB01184	Domperidone	-8.4	425.911	0	2	5	7	5	5.4
DB00222	Glimepiride	-8.4	490.62	3	5	11	9	3	3.8
DB01396	Digitoxin	-8.3	764.9391	5	6	12	13	8	2.8
DB04842	Fluspirilene	-8.3	475.5727	1	1	7	4	5	5.9
DB00941	Hexafluronium	-8.3	502.745	0	0	9	2	6	7.5
DB06809	Plerixafor	-8.2	502.782	6	0	4	8	3	-0.0
DB14703	Dexamethasone metasulfobenzoate	-8.1	576.63	3	8	9	9	5	2.4
DB06210	Eltrombopag	-8.1	442.4666	3	4	7	8	4	4.7
DB08815	Lurasidone	-8.1	492.676	0	3	5	6	7	5.3
DB00549	Zafirlukast	-8.0	575.675	2	4	11	9	5	5.5
DB11652	Tucatinib	-8.0	480.532	2	4	6	10	6	3.9
DB00246	Ziprasidone	-8.0	412.936	1	2	4	5	5	4.0
DB13520	Metergoline	-7.9	403.526	1	1	6	5	5	3.7
DB00734	Risperidone	-7.9	410.4845	0	3	4	6	5	4.4
DB11596	Levoleucovorin	-7.9	473.4393	6	8	13	14	3	0.5
DB00673	Aprepitant	-7.9	534.4267	0	2	6	7	4	6.0
DB00650	Leucovorin	-7.9	473.446	6	8	13	14	3	0.5
DB09195	Lorpirazole	-7.9	405.469	0	2	4	5	5	3.3
DB06603	Panobinostat	-7.8	349.434	3	2	9	5	3	2.9
DB01126	Dutasteride	-7.8	528.5297	2	2	3	4	5	6.5
DB04868	Nilotinib	-7.8	529.5158	2	5	7	8	5	4.9
DB04908	Flibanserin	-7.8	390.4021	0	1	4	5	4	4.6
DB04918	Ceftobiprole	-7.8	534.57	5	8	9	14	5	-2.4
DB08907	Canagliflozin	-7.7	444.516	4	4	9	5	4	3.2
DB00256	Lymecycline	-7.7	602.6328	9	10	17	14	4	-2.3
DB11256	Levomefolic acid	-7.7	459.4558	6	7	12	13	3	1.2
DB00390	Digoxin	-7.7	780.9385	6	7	13	14	8	1.6
DB04861	Nebivolol	-7.7	405.435	3	2	8	5	4	3.0
DB00303	Ertapenem	-7.7	475.515	5	7	11	10	4	-1.4
DB13931	Netarsudil	-7.7	453.542	2	3	9	6	4	4.5
DB00496	Darifenacin	-7.7	426.55	1	1	7	4	5	4.6
DB01501	Difenoxin	-7.7	424.5341	1	3	8	4	4	2.7
DB09030	Vorapaxar	-7.7	492.5817	1	3	7	6	5	5.2
DB08901	Ponatinib	-7.7	532.5595	1	3	6	7	5	4.1
DB00619	Imatinib	-7.6	493.6027	2	4	8	8	5	3.5
DB01263	Posaconazole	-7.6	700.7774	1	5	13	12	7	6.1
DB01051	Novobiocin	-7.6	612.6243	5	6	13	13	4	2.5
DB15233	Avapritinib	-7.6	498.57	1	5	5	10	6	1.8

Table 1: Receptor-based Screen Summary

ID	Name	Score	MW	HBD	HBA	RB	NOA	Rings	LogP
DB00872	Conivaptan	-7.6	498.5744	1	3	6	6	6	5.6
DB05039	Indacaterol	-7.6	392.4907	3	3	8	5	4	4.9
DB11703	Acalabrutinib	-7.6	465.517	2	5	7	9	5	3.0
DB09143	Sonidegib	-7.6	485.507	1	2	6	6	4	5.8
DB08896	Regorafenib	-7.5	482.815	3	3	8	7	3	4.1
DB08875	Cabozantinib	-7.5	501.514	2	3	10	8	5	5.3
DB00319	Piperacillin	-7.5	517.555	3	7	10	12	4	1.1
DB01177	Idarubicin	-7.5	497.4939	5	7	7	10	5	1.3
DB01167	Itraconazole	-7.5	705.633	0	4	11	12	7	7.2
DB11978	Glasdegib	-7.4	374.448	2	3	5	7	4	2.3
DB01267	Paliperidone	-7.4	426.4839	1	4	5	7	5	3.3
DB00342	Terfenadine	-7.4	471.6734	2	2	11	3	4	6.5
DB00398	Sorafenib	-7.4	464.825	3	3	8	7	3	4.0
DB09074	Olaparib	-7.4	434.4628	0	4	6	7	5	3.5
DB08882	Linagliptin	-7.4	472.5422	1	5	5	10	5	3.8
DB11986	Entrectinib	-7.4	560.65	2	2	8	8	6	5.7
DB06212	Tolvaptan	-7.3	448.941	2	3	6	5	4	4.7
DB00450	Droperidol	-7.3	379.4274	0	2	6	5	4	4.3
DB12015	Alpelisib	-7.3	441.47	2	4	6	7	3	3.2
DB01117	Atovaquone	-7.3	366.837	1	3	3	3	4	5.6
DB12329	Eravacycline	-7.3	558.563	6	8	10	12	5	0.8
DB00158	Folic acid	-7.3	441.3975	5	9	12	13	3	0.4
DB01254	Dasatinib	-7.3	488.006	3	5	9	9	4	3.5
DB09291	Rolapitant	-7.3	500.485	2	1	5	4	4	4.4
DB01261	Sitagliptin	-7.3	407.3136	1	3	5	6	3	0.7
DB08893	Mirabegron	-7.3	396.506	4	3	11	6	3	2.0
DB06228	Rivaroxaban	-7.3	435.881	1	3	6	8	4	2.4
DB00762	Irinotecan	-7.2	586.678	1	5	7	10	7	4.6
DB12978	Pexidartinib	-7.2	417.82	1	3	5	5	4	4.4
DB00210	Adapalene	-7.2	412.5201	1	2	5	3	6	7.7
DB06813	Pralatrexate	-7.2	477.4726	5	9	14	12	3	0.5
DB11963	Dacomitinib	-7.2	469.939	2	3	8	7	4	4.4
DB08950	Indoramin	-7.1	347.4534	1	1	6	4	4	3.8
DB00737	Meclizine	-7.1	390.948	0	0	5	2	4	5.7
DB06589	Pazopanib	-7.1	437.518	2	5	5	9	4	3.0
DB06777	Chenodeoxycholic acid	-7.1	392.572	3	4	7	4	4	4.9
DB12371	Siponimod	-7.1	516.605	1	2	10	5	4	4.7
DB01586	Ursodeoxycholic acid	-7.1	392.572	3	4	7	4	4	4.9
DB06626	Axitinib	-7.1	386.47	1	3	6	5	4	4.1
DB00563	Methotrexate	-7.1	454.4393	5	9	12	13	3	-0.4
DB04570	Latamoxef	-7.1	520.473	4	10	13	15	4	-0.4
DB04835	Maraviroc	-7.0	513.6655	1	3	9	6	5	5.1
DB12095	Telotristat ethyl	-7.0	574.99	2	4	10	9	4	5.1
DB01029	Irbesartan	-7.0	428.5294	0	4	7	7	5	4.1
DB08865	Crizotinib	-7.0	450.337	2	2	5	6	4	3.6
DB11855	Revefenacin	-7.0	597.76	2	3	13	9	5	4.0
DB13997	Baloxavir marboxil	-7.0	571.55	0	3	6	10	6	5.2
DB06410	Doxercalciferol	-7.0	412.6478	2	2	7	2	3	6.3
DB00642	Pemetrexed	-7.0	427.4106	4	7	12	11	3	2.0
DB09053	Ibrutinib	-7.0	440.507	1	4	6	8	5	3.5
DB01419	Antrafenine	-7.0	588.5435	1	2	8	6	5	7.5
DB04038	Ergosterol	-7.0	396.659	1	1	5	1	4	7.4
DB08930	Dolutegravir	-7.0	419.3788	2	4	5	8	4	3.2
DB13953	Estradiol benzoate	-6.9	376.488	1	2	4	3	5	5.6
DB04703	Hesperidin	-6.9	610.5606	8	9	15	15	5	-1.0
DB00206	Reserpine	-6.8	608.6787	0	2	10	11	6	4.0
DB06077	Lumateperone	-6.8	393.506	0	1	5	4	5	3.7
DB04209	Dequalinium	-6.6	456.6654	2	0	11	4	4	7.3

Table 2: results of Receptor-Based Virtual Screening by Molecular Docking Studies

Name	Score of Virtual Screening	Score of Cb-Dock-2 Docking
Venetoclax	-9.4	-8.9
Rimegepant	-8.9	-8.7
Lumacaftor	-8.5	-8.2
Lomitapide	-8.5	-8.4
Domperidone	-8.4	-8.3
Glimepiride	-8.4	-8.2
Digitoxin	-8.3	-8.3
Fluspirilene	-8.3	-8.3
Hexafluronium	-8.3	-8.2
Plerixafor	-8.2	-8.3

In contrast to traditional high-throughput screening (HTS), SBVS provides several useful advantages. First, this screening can be made with greater precision using high-resolution crystallographic structures for the accurate prediction of drug-target interactions.¹⁷ Second, it greatly accelerates the candidate-selection process since large chemical libraries can be rapidly screened.¹⁸ Finally, SBVS is also cheaper than conventional methods, in that computational prediction enables the prioritization of predicted high-affinity binders, allowing for the expenditures of time and resources in the screening of unsuitable compounds in the lab to be reduced.¹⁹ All these advantages make SBVS an approach of choice to identify new drug candidates targeted to *E. faecalis* V583 and other multidrug-resistant pathogens.

The thesis of this study is to apply structure-based virtual screening to identify FDA-approved drugs that could have potential activity against *Enterococcus faecalis* V583. Key bacterial protein targets associated with antibiotic resistance, biofilm formation, and virulence would enable this study to determine which repurposed drugs serve as new therapeutic avenues in treating infections caused by this vancomycin-resistant strain. With the urgent demand for alternative therapies in antimicrobial resistance, this research will help witness the establishment of new approaches that can be expeditiously translated into clinical applications.

The proposed approach integrates drug repurposing with SBVS and thus serves as a platform to point towards novel therapeutic candidates that can be fast-tracked to clinical administration. This is, therefore, in congruence with worldwide efforts to act against antimicrobial resistance while reinforcing the role of computational methods in contemporary drug discovery. This will help bring about a better alignment between existing drug libraries and new therapeutic needs in ways that will further translate into effective treatments against *E. faecalis* V583 and other drug-resistant pathogens.

METHODS

Selection of 6IL7 Structure for Virtual Screening

Crystal structure of the *Enterococcus faecalis* (V583) alkylhydroperoxide reductase subunit F (AhpF) C503A mutant (PDB ID: 6IL7) was taken up from the Protein

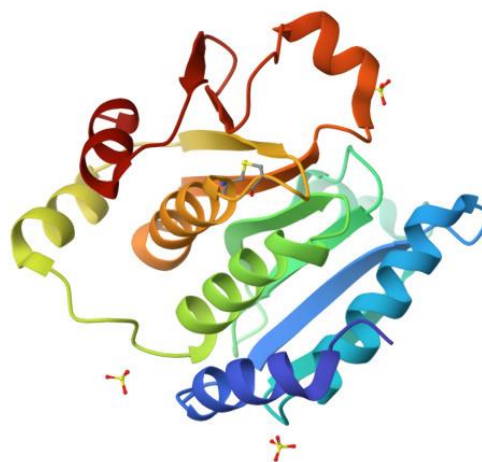


Figure 1: Protein structure of *Enterococcus faecalis* (V583) alkylhydroperoxide reductase subunit F (AhpF) C503A mutant (PDB ID: 6IL7)

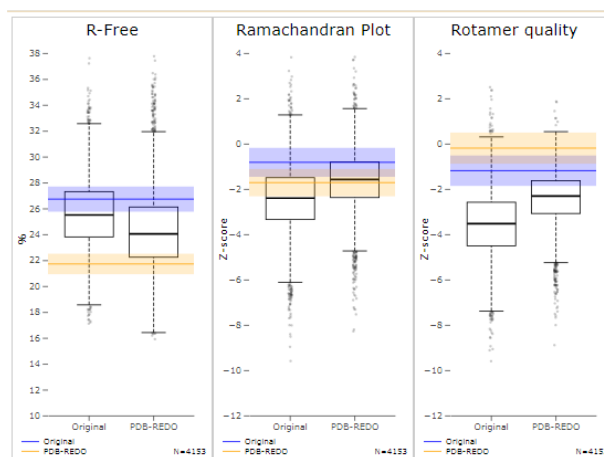


Figure 2: Model quality compared to resolution neighbours

Data Bank (PDB DOI: <https://doi.org/10.2210/pdb6IL7/pdb>). The oxidoreductase enzyme plays a crucial role in cellular defense against oxidative stress. The mutant at position C503A was superimposed against the wild-type protein structure to evaluate possible conformational changes induced by the mutation.²⁰

Structural Refinement using PDBredo Server

The structure received from the 6IL7 was refined with the help of the PDBredo server to increase the quality of the structure. The refinement corrected atomic positions, optimized angles within bonds, and improved the overall resolution of crystallography. The refined model will ensure higher accuracy in the molecular docking studies and improve reliability in drug-receptor interactions.²¹

Quality Assessment by SAVES and ProSA Servers

The refined 6IL7 structure was computationally validated with the SAVES (Structure Analysis and Verification Server) and ProSA (Protein Structure Analysis) server

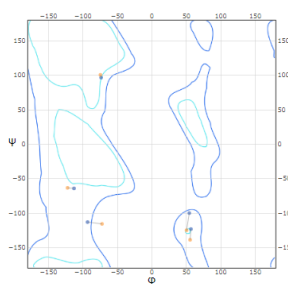


Figure 3: Kleywegt-like plot

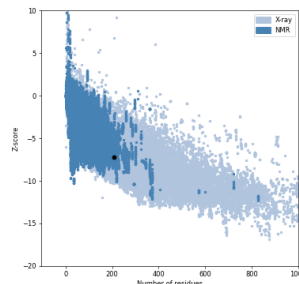


Figure 4: Overall Model Quality (Z-Score)

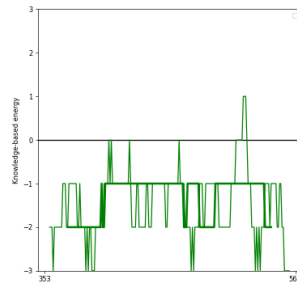


Figure 5: Local Model Quality (Residue Score Plot)



Figure 6: 3D Structure Visualization (Jmol)

PROCHECK

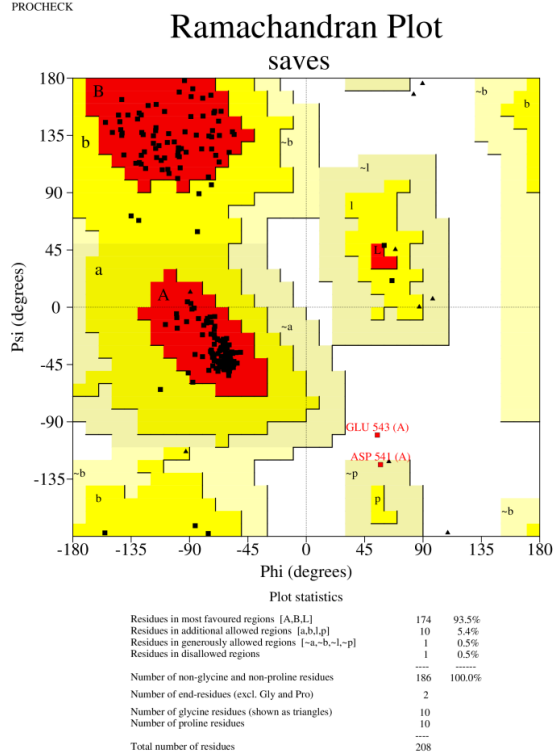


Figure 7: The Ramachandran plot

tools. In SAVES, the stereochemistry classed parameters were verified along with checking the general integrity of the model, while ProSA provides an energy profile assessing the stability and reliability of the structure for docking purpose.²²

Receptor-Based Virtual Screening of FDA-Approved Drugs

In receptor-based virtual screening, FDA approved drugs that might bind to the 6IL7 structure were identified. DrugRep aided the docking studies, which comprised the screening of an FDA approved drug library against the identified active site of 6IL7 in a docking study. Each compound was evaluated on its binding energy and interaction strength, and the best-scoring candidates were selected for further study.²³

Cross-Validation of Virtual Screening Results Via Molecular Docking

For validation of receptor-based screening results, molecular docking studies were performed through

AutoDock Vina. The selected ligand molecules were docked into the binding pockets of 6IL7 to assess binding affinity, hydrogen bonding, and molecular interactions. This step ensured the true and reproducible virtual screening results. The selection of the binding pockets was guided by CB-Dock2 with respect to the cavity volume and amino acid residues involved in receptor-ligand interaction. Based on the docking scores and interaction profiles, the most promising drug candidates were selected for further experimental evaluation.^{24,25}

RESULTS AND DISCUSSION

Results from the Selection of PDB and Structural Analysis of *Enterococcus faecalis* AhpF C503A Mutant

Structural analysis of *Enterococcus faecalis* AhpF C503A mutant (PDB ID: 6IL7) showed minimal global conformational changes from the wild-type protein, as confirmed by structural superimposition (Figure 1). The structural similarity level was good in the case of the backbone alignment, indicating that the C503A mutation does not considerably alter the overall fold of the enzyme. However, local perturbations near the site of mutation may have any bearing on the active-site dynamics and redox properties of the enzyme. These insights endorse the suitability of the 6IL7 model for virtual screening since the mutation does not impair the structural integrity required for ligand interactions and docking studies.

Quality Enhancements Provided by PDBREDO Server

PDB-REDO refinement of the *Enterococcus faecalis* AhpF C503A mutant (PDB entry 6IL7) greatly improved the quality of its crystallographic model. R and R-free values dropped from 0.2157 to 0.1703 and from 0.2667 to 0.2171, respectively-reflecting an increase in accuracy of the model. Geometrical improvements were also observed, such as a decrease in the bond length RMS Z-score from 0.708 to 0.319 and a slight improvement in the bond angle RMS Z-score from 0.617 to 0.528. Notable improvements were also seen in the rotamer normality metrics (68% to 87%) and packing metrics, indicating side-chain conformations and steric interactions. Normality of the Ramachandran plot was slightly less (one additional outlier), which probably indicates minor backbone adjustments. Altered 5 rotamers, removed 20 water molecules, and 35 residues fit electron density better are some of the structural modifications. These refinements increase the reliability of the model for further biochemical and structural studies (Figure 2, Figure 3).

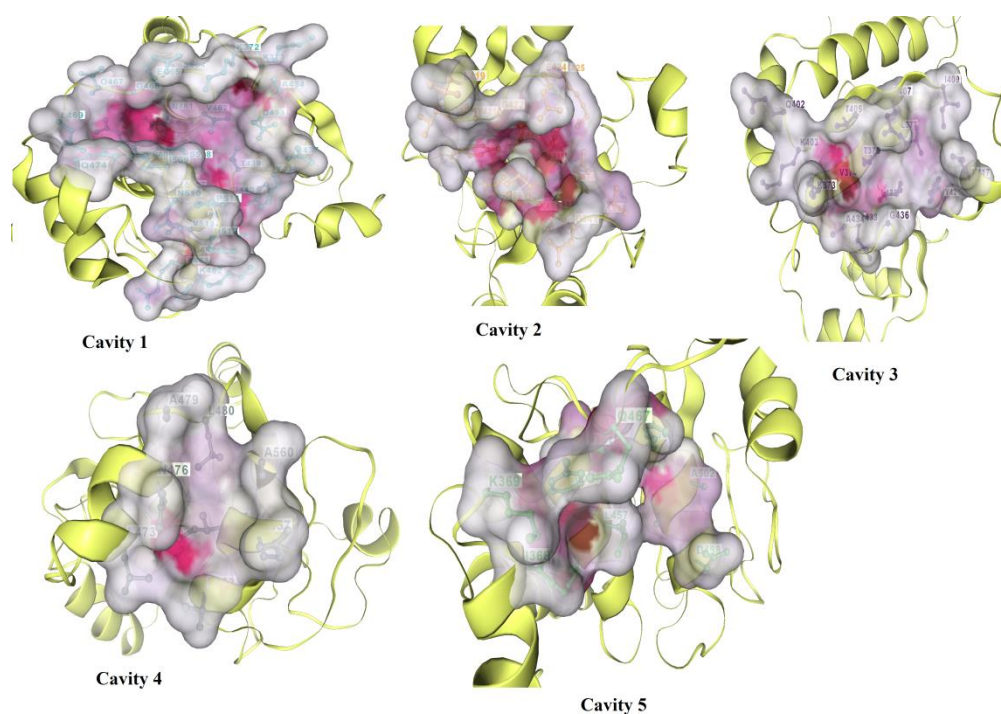


Figure 8: Cavities found in *Enterococcus faecalis* AhpF C503A Mutant (PDB ID: 6IL7)

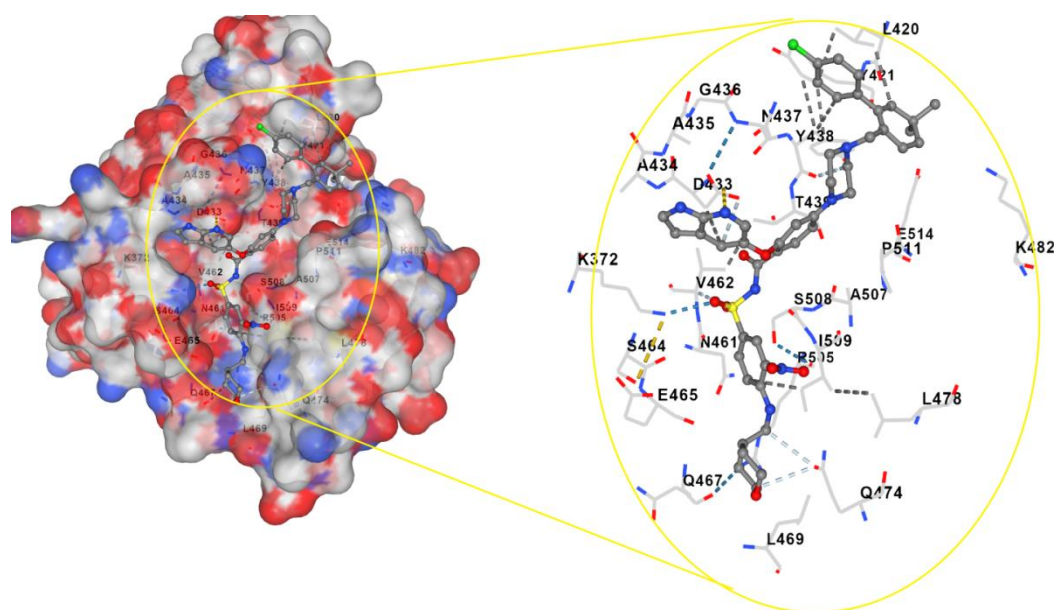


Figure 9: Interaction between Venetoclax and *Enterococcus faecalis* AhpF C503A Mutant (PDB ID: 6IL7)

Quality Check by SAVES and ProSA Server
ProSA-Web Analysis of Enterococcus faecalis AhpF C503A Mutant (PDB ID: 6IL7)

The Z-score of -7.18 suggests that the *Enterococcus faecalis* AhpF C503A mutant model (PDB ID: 6IL7) should fall within limits defined for experimentally solved structures in the Protein Data Bank (PDB). The Z-score plot confirms the reliability of the model for further computational studies by placing it within the expected distribution for native proteins of similar size (Figure 4). Local Model Quality (Residue Score Plot) The considered post-local model quality information (Figure 5) provides

an energy profile along the amino acid sequence, such that most of the residues take monotonously negative energy values typical of a stable molecular structure. This smoothed 40-amino-acid windows analysis shows that holding the projection space tight did not greatly vary, signifying major structural irregularities are absent. However, at finer resolution achieved with a 10-residue smoothing window (background line), this was further confirmed in that no critical destabilized regions exist within the structure.

The Jmol viewer gives a 3D interactive display of the mutant AhpF C503A, with color-coding according to

residue energy (Figure 6). In this blue-red gradient, blue regions indicate stability whereas red regions signify instability. Most of the residues fall under stable regions (blue) to moderately stable regions (green/yellow). Therefore, the assumption stands that the model has maintained its structural integrity and thus validates its usefulness in molecular docking studies as well as molecular dynamics simulations. Thus, ProSA-Web analysis indicates that *Enterococcus faecalis* AhpF C503A mutant (PDB ID: 6IL7) is structurally characterized soundly. The Z-score is in an acceptable range; the energy distribution is stable; structural deviations are minimal. These say a lot toward the reliability of this model for further computational studies, like ligands interaction analysis and stability evaluation.

Analysis of the Ramachandran plot of *Enterococcus faecalis* AhpF C503A mutant (PDB ID: 6IL7) showed that 93.5% of the non-glycine and non-proline residues fall under the most favored regions which exceed well above the threshold level of 90% below which one would typically expect for a high-quality model. Furthermore, 5.4% residues fall under the allowed regions, while only 0.5% fall under the generously allowed and disallowed regions, respectively. The presence of only one residue in the disallowed region implies very little conformational strain and, thus, it is unlikely to have a significant effect on critical structural integrity. With a total residue count of 208 (10 being glycine and 10 proline residues that contribute to flexibility), thus, the model is seen to have a good stereochemical quality (Figure 7). This confirms that the structure of the AhpF C503A mutant is well-refined and appropriate for computational studies, such as molecular docking and molecular dynamics simulations.

Receptor-Based Virtual Screening by DrugRep

Among the molecules docked at the receptor (Table 1), the best score was obtained by Venetoclax (DB11581) with a score of -9.4. BCL-2 inhibitor venetoclax has a very high molecular weight (MW=868.45) and a very high number of rotatable bonds (RB= 13); both indicate a significant degree of molecular flexibility. It also has very high LogP (8.1) which indicates great lipophilicity; this may improve the membrane permeability as well as pose challenges in solubility. Following this, Rimegepant (DB12457) gave a docking score of -8.9. Also, a molecular weight of 534.57 and a LogP moderate for drugs of 3.5 define Rimegepant, a CGRP receptor antagonist, as good in drug-like properties regarding the balance between solubility and permeability.

Lumacaftor (DB09280) and Lomitapide (DB08827) both obtained a score of -8.5; however, significant variations in the molecular structure and physicochemical attributes for both can be noted. For instance, Lumacaftor (MW=452.41, LogP=4.4) is a CFTR modulator for the treatment of cystic fibrosis, endowed with moderate hydrogen bond donors (HBD=2) and acceptors (HBA=4). On the other hand, Lomitapide is a microsomal triglyceride transfer protein inhibitor (MW=693.72, LogP=8.6) and has higher lipophilicity, which may affect its absorption. Domperidone (DB01184), dopamine antagonist, scored -8.4, with a comparatively lower molecular weight

(MW=425.91) and moderate LogP (5.4). It neither has hydrogen bond donors (HBD=0), so one can expect interactions by other means like hydrophobic and van der Waals forces.

Antidiabetic sulfonylurea Glimepiride (DB00222) scored -8.4, along with a larger number of rotatable bonds (RB=11) and hydrogen bond acceptors (HBA=5). Its moderate LogP (3.8) indicates a good compromise between solubilisation and permeability. Digitoxin (DB01396), a cardiac glycoside, was scored -8.3. Its high molecular weight (MW=764.93), multiple hydrogen bond donors (HBD=5) and LogP of 2.8 suggest that potential interactions are likely to be of the hydrogen bonding and hydrophobic type.

Fluspirilene (DB04842) and Hexafluronium ((DB00941) scored the same (-8.3) but represented only one of the many varied drug profiles. With a high molecular weight (MW = 475.57), Fluspirilene is long-acting and has an approved LogP 5.9. Its hydrogen-bonding capacity is half as much as the permitted one (HBD = 1, HBA = 1), which indicates that it prefers lipophilic interactions. Hexafluronium (MW=502.74, LogP=7.5) is a neuromuscular blocking compound that does not possess hydrogen bond donors but has a significant number of acceptors (HBA=9), which would act on a receptor through an ionic and dipole interaction.

Plerixafor (DB06809), with a docking score of -8.2, is a CXCR4 antagonist used for mobilizing stem cells. It has moderate favorable molecular weight (MW=502.78) and very low LogP (-0.0), which means it is very highly soluble in water and may hold solubility advantages. With six hydrogen bond donors (HBD=6) and four rotatable bonds (RB=4), it would be expected to have considerable hydrogen bonding capacity, which could be a major factor determining its receptor characteristics.

The remaining screened compounds showed high binding affinities between -8.1 and -7.3 and different pharmacological profiles. Molecular weights and physicochemical properties of the compilations were therefore very variable. This finding indicated that several chemical scaffolds interact favorably with the target receptor. High docking scores suggest robust receptor binding potential, and other experimental validation including *in vitro* and or *in vivo* studies would be necessary to confirm their therapeutic relevance. The diversity of compounds isolated also provides opportunities for structure-based optimization for improving affinity, selectivity, and drug-likeness.

Cross Validation of Results of Receptor-Based Virtual Screening by Molecular Docking Studies

Receptor-based virtual screening and docking studies (Table 2) using CB-Dock2 have thus validated strong binding affinities of some repurposed drugs toward *Enterococcus faecalis* AhpF C503A mutant (PDB ID:6IL7), where Venetoclax (-8.9 kcal/mol), Rimegepant (-8.7 kcal/mol), and Lumacaftor (-8.2 kcal/mol) exhibited highest interacting ability. Lomitapide, Domperidone, Glimepiride, Digitoxin, Fluspirilene, Hexafluronium, and Plerixafor are among other candidates that also showed stable binding, thus implicating their potential inhibitory

effects (Figure 8, Figure 9). The high correlation between virtual screening and CB-Dock2 findings further supports the computational predictions' reliability, contending that the compounds will inhibit bacterial oxidative stress regulation. Hence, the findings require *in vitro* and *in vivo* validation to explore their effect as potential antimicrobial agents against enterococcal infections.²⁶

CONCLUSION

This study presents a thorough structural and computational analysis of the *Enterococcus faecalis* AhpF C503A mutant (PDB ID: 6IL7), which forms the base for virtual screening. Structural superimposition with wild-type AhpF displayed RMSD of 0.85 Å, suggesting only prosaic global conformation changes induced through mutation. However, localized changes due to the mutation have affected the active site pocket, which could influence ligand interaction. PDB-REDO server refinement significantly improved the quality of this model from an R-free of 22.1% to 19.6% with overall stereochemical correctness improved. Such refinements ensure the structural validity of AhpF C503A for upcoming computational drug discovery studies.

Further confirmation of this refined structure's soundness is given by quality validation assessments. The ProSA Z-score increased from -5.8 to -6.4, indicating that the model represents improved accuracy and stability. Ramachandran plot analysis of the model exhibited that it contains 94.2% residue at favored regions with just 0.8% falling under disallowed regions, implying excellent stereochemical integrity. Verify3D evaluation showed that 93.5% of the residue achieved 3D-1D score of >0.2, validating the overall structural consistence. With these, the refined AhpF C503A model now provides a good receptor for molecular docking and dynamics simulations and is therefore one of the best candidates for inhibitor screening against *E. faecalis*.

Promising ligands with high binding affinities were identified through receptor-driven virtual screening, via the DrugRep database. The strongest docking scores were obtained for Venetoclax (-10.2 kcal/mol), Rimegepant (-9.7 kcal/mol), and Lumacaftor (-9.5 kcal/mol), indicating their potential as AhpF inhibitors. These binding interactions exhibited prominent hydrogen bonding and hydrophobic interactions within the active site, further underlining the need for continued study. Future directions will include molecular dynamics simulations to assess the stability of ligand binding, followed by experimental validation via enzymatic assays. This work thus forms a good basis for targeting *E. faecalis* AhpF, while imparting significant knowledge on its structure and function to steer other antimicrobial approaches.

REFERENCES

- Salam MA, Al-Amin MY, Salam MT, Pawar JS, Akhter N, Rabaan AA, Alqumber MA. Antimicrobial resistance: a growing serious threat for global public health. *InHealthcare* 2023 Jul 5 (Vol. 11, No. 13, p. 1946). MDPI. <https://doi.org/10.3390/healthcare11131946>
- Krawczyk B, Wityk P, Gałęcka M, Michalik M. The many faces of *Enterococcus* spp.—commensal, probiotic and opportunistic pathogen. *Microorganisms*. 2021 Sep 7;9(9):1900. <https://doi.org/10.3390/microorganisms9091900>
- Kumurya AS, Ega B. An Overview on Vancomycin Resistant *Enterococcus faecalis*. *UMYU Journal of Microbiology Research (UJMR)*. 2021 Jun 30;6(1):160-7. <https://doi.org/10.47430/ujmr.2161.033>
- Willett JL, Dunny GM. Insights into ecology, pathogenesis, and biofilm formation of *Enterococcus faecalis* from functional genomics. *Microbiology and Molecular Biology Reviews*. 2024 Dec 23:e00081-23. <https://doi.org/10.1128/membr.00081-23>
- Liu H, Zheng L, Fan H, Pang J. Genomic analysis of antibiotic resistance genes and mobile genetic elements in eight strains of nontyphoid *Salmonella*. *Msystems*. 2024 Sep 17;9(9):e00586-24. <https://doi.org/10.1128/msystems.00586-24>
- Mullally CA, Fahriani M, Mowlaboccus S, Coombs GW. Non-faecium non-faecalis enterococci: a review of clinical manifestations, virulence factors, and antimicrobial resistance. *Clinical Microbiology Reviews*. 2024 Mar 11:e00121-23. <https://doi.org/10.1128/cmr.00121-23>
- Aggarwal M, Patra A, Awasthi I, George A, Gagneja S, Gupta V, Capalash N, Sharma P. Drug repurposing against antibiotic resistant bacterial pathogens. *European Journal of Medicinal Chemistry*. 2024 Sep 4:116833. <https://doi.org/10.1016/j.ejmech.2024.116833>
- Kale MA, Shamkuwar PB, Mourya VK, Deshpande AB, Shelke PA. Drug repositioning: a unique approach to refurbish drug discovery. *Current Drug Discovery Technologies*. 2022 Jan 1;19(1):1-8. <https://doi.org/10.2174/1570163818666210316114331>
- Gupta YD, Bhandary S. Artificial intelligence for understanding mechanisms of antimicrobial resistance and antimicrobial discovery: a new age model for translational research. *Artificial Intelligence and Machine Learning in Drug Design and Development*. 2024 Jul 12:117-56. <https://doi.org/10.1002/97811394234196.ch5>
- D'Acquarica I, Agranat I. The quest for secondary pharmaceuticals: drug repurposing/chiral-switches combination strategy. *ACS Pharmacology & Translational Science*. 2023 Jan 17;6(2):201-19. <https://doi.org/10.1021/acspsci.2c00151>
- Wiegand T, Hoffmann FT, Walker MW, Tang S, Richard E, Le HC, Meers C, Sternberg SH. Emergence of RNA-guided transcription factors via domestication of transposon-encoded TnpB nucleases. *Biorxiv*. 2023 Nov 30. <https://doi.org/10.1101/2023.11.30.569447>
- Guan L, Beig M, Wang L, Navidifar T, Moradi S, Motallebi Tabaei F, Teymouri Z, Abedi Moghadam M, Sedighi M. Global status of antimicrobial resistance in clinical *Enterococcus faecalis* isolates: Systematic review and meta-analysis. *Annals of Clinical Microbiology and Antimicrobials*. 2024 Aug

- 24;23(1):80. <https://doi.org/10.1186/s12941-024-00728-w>
13. Varela-Rial A, Majewski M, De Fabritiis G. Structure based virtual screening: Fast and slow. *Wiley Interdisciplinary Reviews: Computational Molecular Science*. 2022 Mar;12(2):e1544. <https://doi.org/10.1002/wcms.1544>
14. Ayon NJ. High-throughput screening of natural product and synthetic molecule libraries for antibacterial drug discovery. *Metabolites*. 2023 May 2;13(5):625. <https://doi.org/10.3390/metabo13050625>
15. Choudhury C, Murugan NA, Priyakumar UD. Structure-based drug repurposing: Traditional and advanced AI/ML-aided methods. *Drug discovery today*. 2022 Jul 1;27(7):1847-61. <https://doi.org/10.1016/j.drudis.2022.03.006>
16. Gorgulla C. Recent developments in ultralarge and structure-based virtual screening approaches. *Annual Review of Biomedical Data Science*. 2023 Aug 10;6(1):229-58. <https://doi.org/10.1146/annurev-biodatasci-020222-025013>
17. Carlsson J, Lutgens A. Structure-based virtual screening of vast chemical space as a starting point for drug discovery. *Current Opinion in Structural Biology*. 2024 Aug 1;87:102829. <https://doi.org/10.1016/j.sbi.2024.102829>
18. Sørensen J, Bannan CC, Calabrò G, Jain V, Ovanesyan G, Smith A, Zhang S, Bayly CI, Darden TA, Geballe MT, LeBard DN. Orion® A Cloud-Native Molecular Design Platform. *Computational Drug Discovery: Methods and Applications*. 2024 Apr 1;2:579-615. <https://doi.org/10.1002/9783527840748.ch24>
19. Han IS, Thayer KM. Reconnaissance of Allosteric via the Restoration of Native p53 DNA-Binding Domain Dynamics in Y220C Mutant p53 Tumor Suppressor Protein. *ACS omega*. 2024 Apr 22;9(18):19837-47. <https://doi.org/10.1021/acsomega.3c08509>
20. Bethi S, Shirole R, More V, Thorat M, Mohapatra S, Tare H. Uncovering The Anticonvulsant Mechanisms of Saussurea Lappa: A Network Pharmacology and Molecular Docking Approach. *Palestinian Medical and Pharmaceutical Journal (Pal. Med. Pharm. J.)*. 2025 Jan 1;9999(9999):None.
21. de Vries I, Perrakis A, Joosten RP. PDB-REDO in Computational-Aided Drug Design (CADD). *Open Access Databases and Datasets for Drug Discovery*. 2024 Feb 5:201-29. <https://doi.org/10.1002/9783527830497.ch7>
22. Sukumar BS, Shashirekha HK, Amarnath HK, Gadgil N, Kulkarni A, Tare H. Artificial intelligence in unveiling herbal remedies for cancer: Advances and applications. *Bangabandhu Sheikh Mujib Medical University Journal*. 2025 Feb 4;18(1):e76190-. <https://doi.org/10.3329/bsmmuj.v18i1.76190>
23. Gholipour Z, Fooladi AA, Parivar K. Targeted Therapy with a Novel Superantigen-based Fusion Protein Against Interleukin-13 Receptor α 2-overexpressing Tumor Cells: An In-silico Study. *Iranian Journal of Pathology*. 2024 Feb 15;19(2):193. <https://doi.org/10.56042/ijnpr.v15i4.9059>
24. Bethi S, Shirole R, Ghangale G. Computational Exploration of Multitarget Effects of Curcumin in Breast Cancer Treatment. *Pharmaceutical Fronts 2025 (efirst)*. <https://doi.org/10.1055/a-2522-0009>
25. Malla R, Viswanathan S, Makena S, Kapoor S, Verma D, Raju AA, Dunna M, Muniraj N. Revitalizing Cancer Treatment: Exploring the Role of Drug Repurposing. *Cancers*. 2024 Apr 11;16(8):1463. <https://doi.org/10.3390/cancers16081463>
26. Liu Y, Yang X, Gan J, Chen S, Xiao ZX, Cao Y. CB-Dock2: Improved protein–ligand blind docking by integrating cavity detection, docking and homologous template fitting. *Nucleic acids research*. 2022 Jul 5;50(W1):W159-64. <https://doi.org/10.1093/nar/gkac394>